

Reliable measurement of near-critical adsorption by gravimetric method

Ronny Pini · Stefan Ottiger · Arvind Rajendran ·
Giuseppe Storti · Marco Mazzotti

© Springer Science + Business Media, LLC 2006

Abstract A gravimetric apparatus is used to measure the excess adsorption at high pressure. The equipment consists of a Rubotherm magnetic suspension balance, which allows to measure also the density of the fluid. In order to obtain the excess adsorbed amount, the measured weight has to be corrected with a buoyancy term, for which the density of the adsorbing fluid has to be known at each experimental conditions. Therefore the homogeneity of density in the high-pressure cell plays a fundamental role in determining the accuracy of the measured excess adsorbed amounts. This paper is intended to show the impact of the actual approach to thermostating the unit on the density distribution of the adsorbing fluid inside the high-pressure cell. Namely, by changing the inlet position of the heating fluid, large differences in the measured excess adsorption are produced. The closer to the critical point of the fluid, the

stronger are these differences. An optimum configuration for our measuring device has been found and it has been used to study the adsorption of carbon dioxide (CO₂) on Filtrasorb 400 activated carbon at supercritical and near-critical conditions.

Keywords Supercritical CO₂ · Gravimetric method · Near-critical adsorption · Activated carbon

1 Introduction

Measuring high-pressure adsorption is a challenging task. The two most popular approaches used to measure adsorption are the volumetric and the gravimetric methods (Sircar, 2001). In this study a device based on the gravimetric technique is used. It is a magnetic suspension balance from Rubotherm (Bochum, Germany), that has been used for high-pressure adsorption measurements of several gases on different adsorbents in our laboratory (Di Giovanni et al., 2001; Hocker et al., 2003; Rajendran et al., 2002). This instrument allows to measure the weight of a suspended basket containing the adsorbent and the density of the fluid bulk phase with the help of a calibrated sinker (Dreisbach and Lösch, 2000). From these two quantities, the excess adsorption is readily evaluated. Moreover, the density measurement avoids the use of an equation of state to estimate the fluid density from pressure and temperature measurements. Due to the non-applicability of typical equations of state close to the critical point, the di-

R. Pini, S. Ottiger · A. Rajendran · M. Mazzotti (✉)
ETH Zurich, Institute of Process Engineering,
Sonneggstrasse 3, CH-8092 Zurich, Switzerland
e-mail: marco.mazzotti@ipe.mavt.ethz.ch

G. Storti
ETH Zurich, Institute for Chemical and Bioengineering,
Wolfgang-Pauli-Str. 10, CH-8093 Zurich, Switzerland

A. Rajendran
Present address:
School of Chemical and Biomedical Engineering, Nanyang
Technological University (NTU), Blk 1 Innovation Centre,
16 Nanyang Drive, Singapore 637722

rect density measurement becomes extremely valuable for measuring near critical adsorption. On the other hand, it is important that the system is homogeneous, i.e. that temperature and pressure are identical everywhere in the measuring cell to ensure accurate density measurement. Since pressure homogenization is fast and easy, it is important that temperature gradients are as small as possible inside the measuring cell. Among the several requirements to establish such conditions, the careful design of the heating system of the device is an important one. In fact, it is well known that the phase behavior of gases like carbon dioxide is strongly dependent on temperature, especially in the near-critical region.

In the past, several effects were observed in our laboratory when measuring near-critical isotherms by the gravimetric method, namely critical adsorption (Hocker et al., 2003) and critical depletion (Rajendran et al., 2002). However, anomalous behaviors in the near-critical region were also observed by other authors. The adsorption of CO₂ on Filtrasorb 400 activated carbon has been investigated by Tomasko and his group (Humayun and Tomasko, 2000). They found that at a temperature of 32°C the isotherm was exhibiting a “bump” around the critical density, differently from the isotherms measured at higher temperatures, where an almost linear behavior was found in the same density range. Another phenomenon, called critical depletion, was presented for the first time by Findenegg and coworkers for the case of SF₆ on graphitized carbon black using a volumetric adsorption apparatus (Thommes et al., 1994). The phenomenon of critical depletion was then further confirmed by adsorption measurements of the same adsorbate on controlled pore glasses CPG-350 (Thommes et al., 1995) and CPG-100 (Machin, 1999). Several attempts to theoretically explain critical depletion have been proposed by the same authors. Although such theoretical arguments appeared to reasonably explain it (Schoen and Thommes, 1995; Schoen et al., 1997; Thommes et al., 1995), it was shown later that this behavior was due to a simulation artifact (Wilding and Schoen, 1999). Other authors tried some modeling of critical depletion (Kiselev and Ely, 2004; Kiselev et al., 2000, 1999; Maciolek et al., 1998, 1999), however no conclusive explanation of the phenomenon has been found yet. It is therefore still unclear if critical depletion is a real phenomenon and which requirements the adsorbent has to fulfill to exhibit such behavior.

The focus of this work is the analysis of the impact of the heating system on the measurement results. Namely, the effect of different feeding arrangements of the thermostating circuit on the response of the measuring device (in terms of stability and measurement accuracy) has been studied, with emphasis on measuring excess adsorption isotherms in the vicinity of the critical point. The analysis is carried out with reference to a practical case, i.e. near-critical adsorption of CO₂ on a Filtrasorb 400 activated carbon.

2 Experimental section

2.1 Materials

Activated carbon (Filtrasorb 400, mesh 12 × 40, Batch Nr. FE 90623B) was obtained from Chemviron Carbon (Neu-Isenburg, Germany). According to the manufacturer the size of the particles was between 0.6 and 0.7 mm. Prior to the experiments, the activated carbon was washed in demineralized water in order to remove the fines. Subsequently, the adsorbent was dried under nitrogen at 250°C for two days. The gases used in this study were obtained from Pangas AG (Luzern, Switzerland), namely CO₂ at a purity of 99.995% and He at a purity of 99.999%. The critical properties of the adsorbates are as follows: $T_c(\text{He}) = 5.26 \text{ K}$, $P_c(\text{He}) = 2.26 \times 10^5 \text{ Pa}$, $\rho_c(\text{He}) = 69.3 \text{ kg/m}^3$, $T_c(\text{CO}_2) = 304.1 \text{ K}$, $P_c(\text{CO}_2) = 73.7 \times 10^5 \text{ Pa}$, $\rho_c(\text{CO}_2) = 467.6 \text{ kg/m}^3$.

2.2 Set-up

The adsorption measurements were performed in magnetic suspension balances (Rubotherm, Germany) which, besides the excess adsorbed amount, allow to measure the density of the fluid in-situ (Dreisbach and Löscher, 2000). In this study, two different models of the magnetic suspension balance from the same producer have been used. The first model has been operated since 1999, whereas the second model corresponds to a newer version (2004). Both versions are based on the same gravimetric measurement principle, but they differ in some design aspects. More precisely, the heights of the measuring cells are different (larger in the newer version) and the fluid feed and outlet are positioned differently. Moreover, while the newer version is operated without any major changes, the older version

experienced some modifications during the past years. Among others, to improve the heat transfer, the space between the high-pressure cell and the heating jacket has been filled with fitting copper parts, whereas in the newer version this space is empty. Unless stated otherwise, the main part of the measurements reported in this work were carried out using the older version of the magnetic suspension balance. Maximum values of pressure and temperature are 450 bar and 250°C, respectively, and the weight of the sample is measured with an accuracy of 0.01 mg. The balance is kept at a constant temperature with two heating jackets (one for the suspension coupling and one for the measuring cell), and the temperature is measured with a calibrated thermocouple with an accuracy of 0.1°C. The balance consists of a permanent magnet to which a basket containing the sorbent and a titanium sinker element (whose volume is calibrated) are suspended. The permanent magnet is magnetically coupled to an electric magnet outside the high-pressure cell and it is connected to the control system. The distance between the two magnets is a measure of the weight of the system. The balance readings are obtained at two balance positions. In position 1, the basket alone is lifted while the sinker is at rest. In position 2, both basket and sinker are lifted. Figure 1 shows schematically the different working positions of the balance.

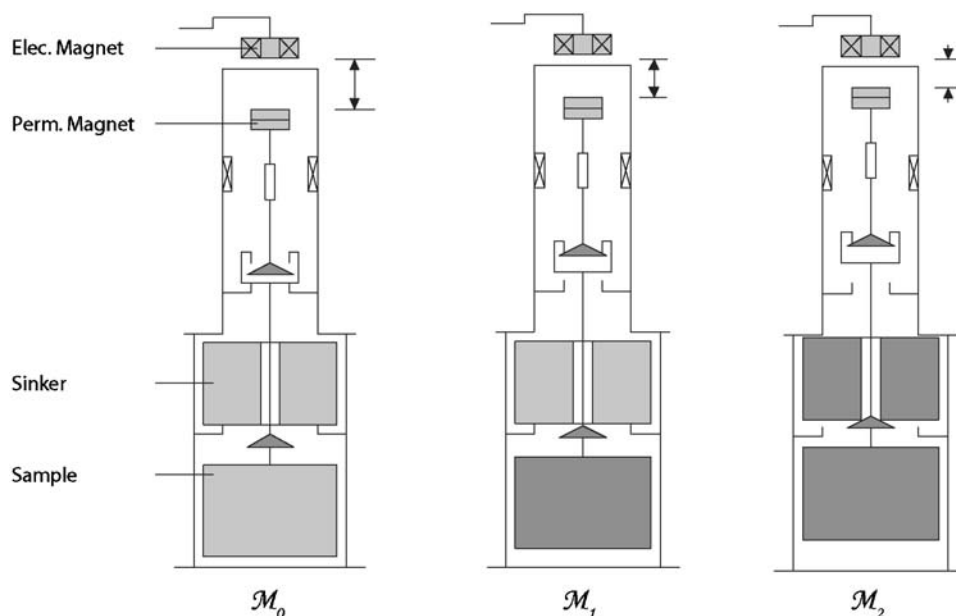


Fig. 1 Different working positions of the magnetic suspension balance from Rubotherm (Bochum, Germany).

Summarizing, two measurements are carried out at two different positions in the cell. To evaluate the adsorption excess then, it is very important that the conditions in the different locations are the very same in terms of temperature and density. More information about the measuring procedure can be found elsewhere (Di Giovanni et al., 2001; Rajendran et al., 2002).

2.2.1 Equations for adsorbing systems

This section reports the equations used to calculate the excess adsorbed amount, $\Gamma(\rho^b, T)$, and the density of the bulk phase, ρ^b in the presence of an adsorbent. These two values are calculated coupling the two equations describing the basket and the sinker, respectively. The underlying assumption is that the bulk density is the same in the two positions.

Basket equation (calculation of the excess adsorbed amount):

$$\Gamma(\rho^b, T) = \mathcal{M}_1(\rho^b, T) - \mathcal{M}_1^0 + \rho^b V^0, \quad (1)$$

where $\mathcal{M}_1(\rho^b, T)$ and \mathcal{M}_1^0 are the weight measured at the desired density ρ^b and temperature T , and under vacuum at high temperature, respectively. The last term in Eq. (1) represents the buoyancy and V^0 the volume of the adsorbent and metal parts (measured

with helium). The procedure for the estimation of both \mathcal{M}_1^0 and V^0 have been extensively explained elsewhere (Di Giovanni et al., 2001).

Sinker equation (calculation of the density):

For the sinker, an equation similar to Eq. (1) can be used. The left-hand side of the equation is zero in this case, because the adsorption on the sinker surface can be neglected.

$$0 = \mathcal{M}_{\text{Sk}}(\rho^b, T) - \mathcal{M}_{\text{Sk}}^0 + \rho^b V^{\text{Sk}}. \quad (2)$$

V^{Sk} is the calibrated volume of the sinker as given by the producer of the instrument. The weight of the sinker $\mathcal{M}_{\text{Sk}}(\rho^b, T)$ at the specific density ρ^b and temperature T is defined as the difference between the balance readings in position 2, $\mathcal{M}_2(\rho^b, T)$, and position 1, $\mathcal{M}_1(\rho^b, T)$. Through this definition and rearranging for the density, the following equation is obtained from Eq. (2):

$$\rho^b = \frac{\mathcal{M}_{\text{Sk}}^0 + \mathcal{M}_1(\rho^b, T) - \mathcal{M}_2(\rho^b, T)}{V^{\text{Sk}}}. \quad (3)$$

Thanks to the two balance readings, $\mathcal{M}_1(\rho^b, T)$ and $\mathcal{M}_2(\rho^b, T)$, the system is therefore completely described by Eqs. (1) and (3) and the excess adsorption is calculated.

2.2.2 Equations for non-adsorbing systems

The same equations described above are now adapted to the case of measurements with empty basket, i.e. without adsorbent. These measurements are actually performed to check if the constant density assumption is valid. Accordingly, different symbols will be used in the following to indicate the density measured in the basket position (ρ_B^b) and the one in the sinker position (ρ_{Sk}^b).

Without adsorbent in the basket and neglecting adsorption on the cell walls, the excess adsorption $\Gamma(\rho^b, T)$ is always equal to zero. By setting the left-hand side of Eq. (1) to zero and replacing ρ^b by ρ_B^b , the basket equation becomes:

$$0 = \mathcal{M}_1(\rho_B^b, T) - \mathcal{M}_1^0 + \rho_B^b V^0, \quad (4)$$

and the following expression for ρ_B^b is obtained:

$$\rho_B^b = \frac{\mathcal{M}_1^0 - \mathcal{M}_1(\rho_B^b, T)}{V^0}. \quad (5)$$

Since \mathcal{M}_1^0 and V^0 are known and $\mathcal{M}_1(\rho_B^b, T)$ is measured, the density can be easily calculated. On the other hand, the same property can be estimated by the sinker equation:

$$\rho_{\text{Sk}}^b = \frac{\mathcal{M}_{\text{Sk}}^0 + \mathcal{M}_1(\rho_{\text{Sk}}^b, T) - \mathcal{M}_2(\rho_{\text{Sk}}^b, T)}{V^{\text{Sk}}}, \quad (6)$$

where the density value in the specific position is involved. If the system is truly homogeneous these two density values are equal.

Following the previous treatment, it becomes clear that a density gradient produces a non-zero value of the excess adsorbed amount, Γ^* , given by:

$$\Gamma^* = \mathcal{M}_1(\rho_B^b, T) - \mathcal{M}_1^0 + \rho_{\text{Sk}}^b V^0 = \Delta\rho V^0. \quad (7)$$

Therefore, the fictitious excess Γ^* is proportional to the density difference $\Delta\rho = \rho_{\text{Sk}}^b - \rho_B^b$. In the specific case where no difference in density is observed, Γ^* is equal to zero and this will be defined as the “ideal” case.

In general, the gas density is strongly affected by temperature. Moreover, such sensitivity becomes very large at near-critical conditions, where minor changes in temperature lead to large differences in density. Therefore, it is obvious that an accurate temperature control is an essential requisite to reliable measurements under these conditions.

3 Results and discussion

3.1 Non-adsorbing system

The heating system of the balance under examination consists of two double wall jackets (one for the suspension coupling and one for the measuring cell). An oil from the same thermostat circulates through both jackets. In principle, the two jackets can be connected to the thermostat to form a parallel or a serial oil circuit. Moreover, an additional degree of freedom is the first position at which the fluid from the thermostat flows in. Therefore, six different configurations can be arranged: Parallel Down (PD) and Up (PU), Serial Down (SD) and Up (SU), Middle Feed (MF) and Outlet (MO). They are schematically shown in Fig. 2, where the acronyms defined above are used. All these different configurations have been checked

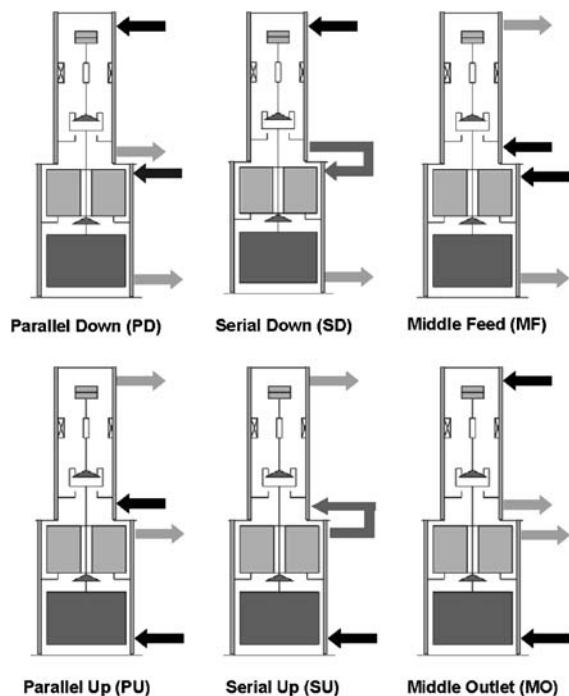


Fig. 2 Different oil-feed configurations for the balance thermostatement. Arrows represent the thermostat fluid directions

experimentally under non-adsorbing conditions and comparatively evaluated in terms of fictitious excess adsorption isotherms. Different temperatures have been selected ranging from far (45°C and 60°C) to near-critical conditions (31.4°C), where large sensitivity is

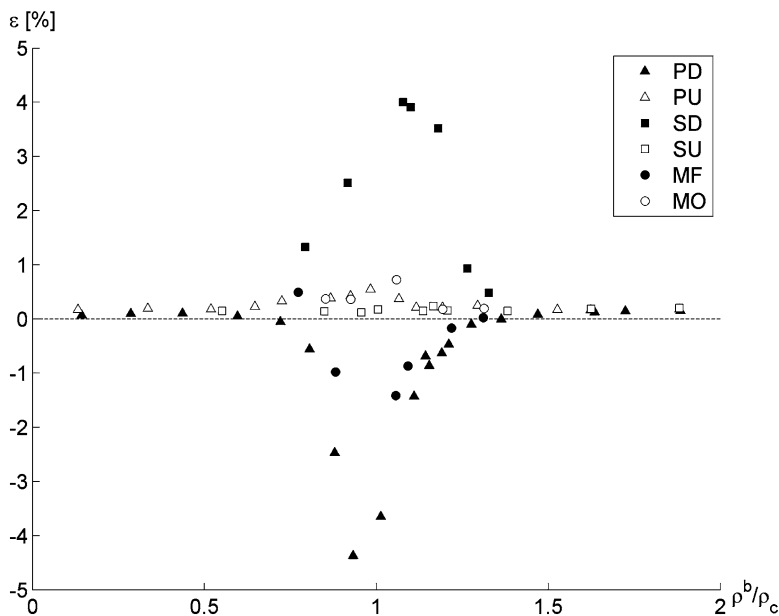
expected. At each pressure, the fictitious excess adsorption Γ^* is calculated using Eq. (7) and $\Delta\rho$ from Eqs. (5) and (6). Finally, the comparison among the different configurations is made in terms of the following relative error:

$$\epsilon = \frac{\rho_B^b - \rho_{Sk}^b}{\rho_B^b} \tag{8}$$

Accordingly, the smaller the error, the larger the homogeneity of conditions inside the cell.

In Fig. 3 such error ϵ is shown against the reduced density, i.e. the density of the bulk phase ρ_{Sk}^b divided by the critical density of the fluid ρ_c . All measurements are carried out using CO₂ as bulk fluid and at 31.4°C, a temperature near the critical temperature of CO₂ (31.0°C). Notably, the error behavior is very different and even opposite, for the different configurations. For example, the two configurations PD and MF lead to negative relative errors ϵ in the vicinity of the critical density, whereas all the other configurations show positive ϵ values in the whole density range. Moreover, for the two configurations PD and SD, this error is large and spans the reduced density range between 0.8 and 1.3 with a maximum value of about 4–5% near the critical density. The only three configurations where this error is always below 1% are those indicated by the empty symbols, namely MO, PU and SU.

Fig. 3 System without adsorbent: error ϵ in the density measurement as a function of the reduced density ρ^b/ρ_c . Temperature 31.4°C



Beside such errors other criteria have been used in order to rank the different configurations. As an example, in the SU-configuration, although the error is very small, a strong instability of the weight measurement has been verified when approaching the critical density, preventing reliable measurements. This effect is probably due to the strong mixing imposed by this configuration, which is maximizing the temperature gradient from the bottom to the top of the cell. A similar situation was observed also in the MO-configuration: here the balance was able to achieve stable signals, but at the expense of very large measurement times. The PU-configuration, indeed, seems to be the best one: the weight measurement is stable and the errors are relatively small over the complete density range. For the reasons mentioned above, we believe that the PU-configuration is a promising arrangement for measuring CO_2 adsorption isotherms in a wide temperature range.

Let us now focus on the two configurations that have been studied in a more detailed way, PU and PD. CO_2 adsorption isotherms on activated carbon have been measured in the past using the last configuration (Ottiger et al., 2005). For both configurations, the relative density error ϵ is plotted in Fig. 4 against the reduced density ρ^b/ρ_c . This plot highlights the temperature dependence of the measured error ϵ for the two configurations. In the PU case (represented by the empty symbols) this error is always small and a temperature dependence cannot be clearly distinguished.

However, in the PD case at 31.4°C and near the critical density a sharp peak appears, indeed not measured at the other two temperature values. This result is considered the ultimate proof that the PU-configuration is the optimal one for measuring high pressure adsorption isotherms using the specific balance under examination.

3.2 Adsorbing system - CO_2 on activated carbon

In order to elucidate the impact of the density error on the adsorption measurements, the system CO_2 on activated carbon Filtrasorb 400 is analyzed in the following. These measurements are limited to the three configurations PD, SD and PU. First, the adsorption isotherms measured at 31.4°C are presented and analyzed for all three configurations, then, a wider temperature range is analyzed using the optimal PU-configuration.

3.2.1 Near-critical measurements

The results of the measurements in the PD-configuration are presented in Fig. 5. The excess adsorption n^{ex} (left vertical scale) and the density difference $\Delta\rho$ (right vertical scale) are shown as a function of the reduced density ρ^b/ρ_c . The correspondence between the peak measured near the critical density of the fluid in the experiment without adsorbent and the anomalous behavior of the isotherm on activated

Fig. 4 System without adsorbent: error ϵ in the density measurement as a function of the reduced density ρ^b/ρ_c and different temperatures for configurations PD and PU

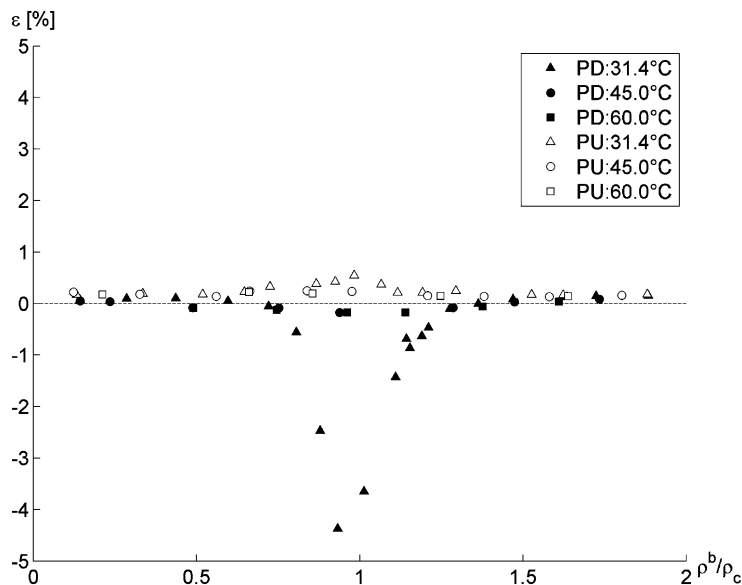
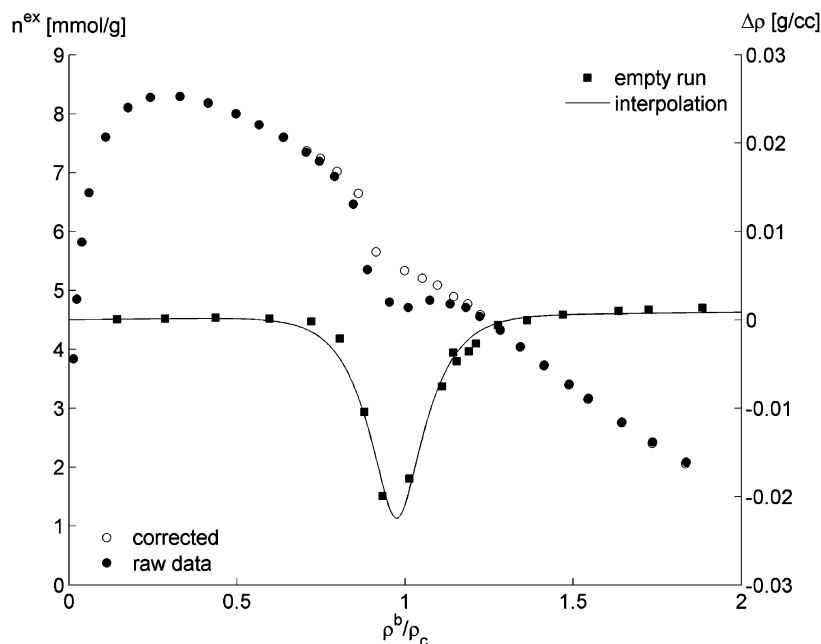


Fig. 5 Excess adsorption isotherms of CO₂ on activated carbon (left y-axis) as a function of the reduced density ρ^b/ρ_c . Density difference $\Delta\rho$ (right y-axis) as a function of the reduced density ρ^b/ρ_c . Configuration PD, temperature 31.4°C



carbon in the same reduced density range (full symbols) is rather convincing. In other words, we believe that the irregular behavior of the measured isotherm is due to the density error.

As additional check of this statement, the following effective approach has been applied: (i) from the empty run, a set of density values at each pressure-temperature conditions is estimated; (ii) these values are used when calculating the excess adsorption using Eq. (1) in the adsorption experiment. The resulting “corrected” isotherm is plotted in Fig. 5 using empty symbols. First of all, this correction cancels almost completely the irregular behavior observed in the measured excess near the critical point. Secondly, this correction is important only in the vicinity of the critical point of the fluid (0.8–1.2 reduced density). Thus concluding, the reported results show convincingly that the irregular behavior of the excess curve vs. reduced density is an artifact related to the measurement technique.

For the SD-configuration, the same approach has been applied. Unlike all the other measurements presented in this paper, the isotherms showed in Fig. 6 have been measured in a different balance, namely the second model described previously. For this reason the data measured without adsorbent in the basket presented in Fig. 6 are different from those corresponding to the same configuration in Fig. 3.

The measured isotherm (raw data), the density difference measured with the empty run and the corrected isotherm are shown in Fig. 6. In contrast to the previous case, the measured density difference is always positive, with a peak in the reduced density range in the vicinity of the critical density of the fluid ($\rho^b/\rho_c = 1$). If we correct the raw data with the new density values estimated from the measurements without adsorbent, a new isotherm is obtained that differs from the original one only in the region near the critical density. The slight bump observed in the original isotherm has now disappeared.

As already mentioned, the PU-configuration appears to be the best one for the specific balance under study: the balance readings are stable and the relative density errors measured with this configuration were considerably smaller than in all the remaining configurations. The same analysis presented for the PD- and SD-configurations is finally presented also for this configuration. In Fig. 7 the measured isotherm (raw data), the density differences measured with the empty run and the corrected isotherm are shown. All the favorable characteristics of this configuration mentioned above are found once more, being the effect of the density correction practically negligible. Under these conditions the equipment can be used without the need of empty runs, thus saving time and effort without losing accuracy.

Fig. 6 Excess adsorption isotherms of CO₂ on activated carbon (left y-axis) as a function of the reduced density ρ^b/ρ_c . Density difference $\Delta\rho$ (right y-axis) as a function of the reduced density ρ^b/ρ_c . Configuration SD, temperature 31.4°C

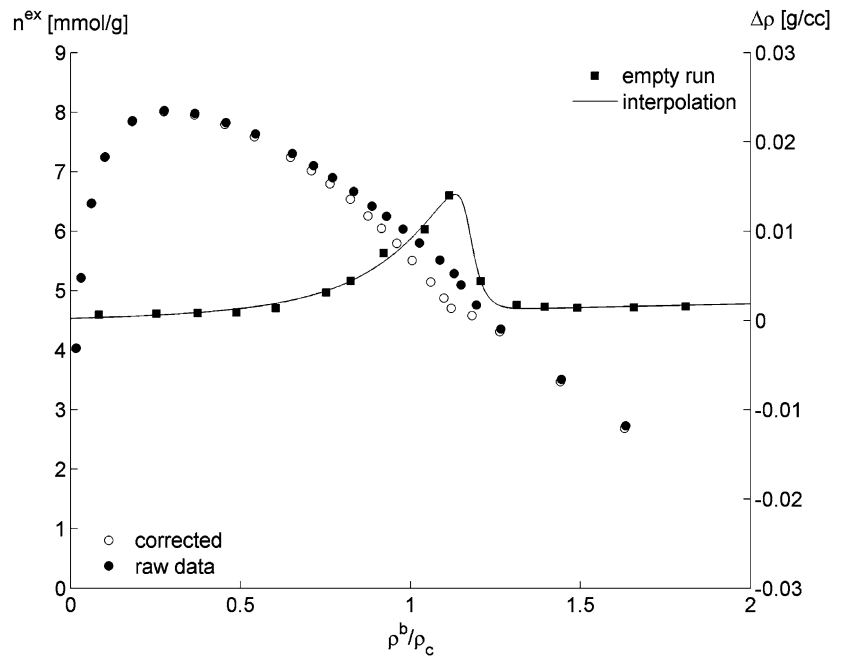
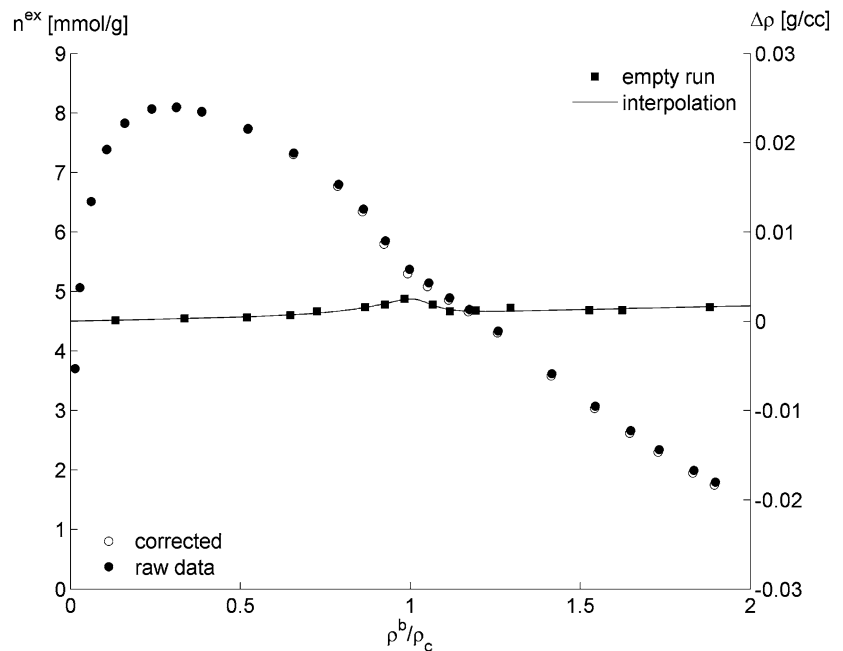


Fig. 7 Excess adsorption isotherms of CO₂ on activated carbon (left y-axis) as a function of the reduced density ρ^b/ρ_c . Density difference $\Delta\rho$ (right y-axis) as a function of the reduced density ρ^b/ρ_c . Configuration PU, temperature 31.4°C



3.2.2 Measurements over a wider temperature range

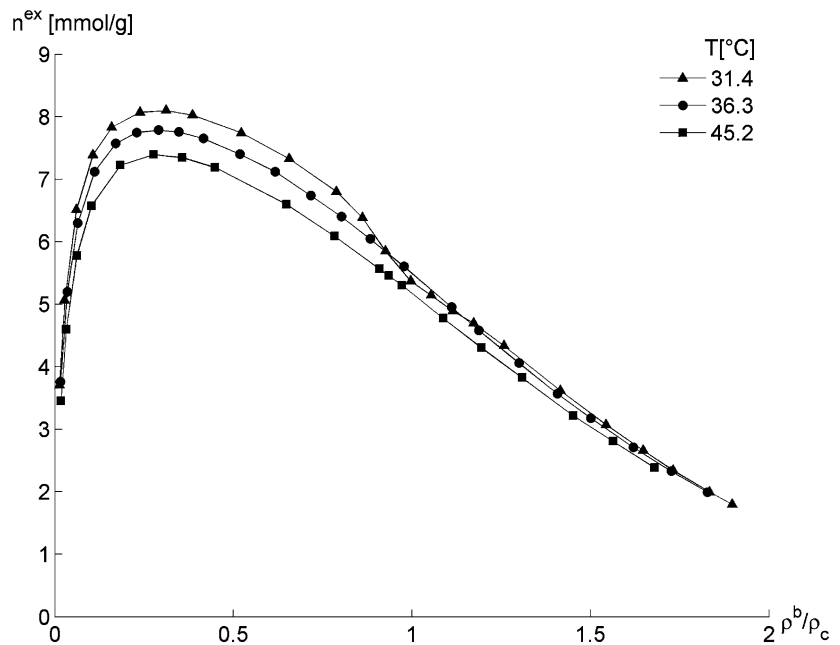
In this section we analyze more in detail the adsorption of CO₂ on activated carbon at different temperatures, by reporting isotherms measured using the PU-configuration. In Fig. 8, the excess adsorption of

CO₂ on Filtrasorb 400 is shown against the reduced density ρ^b/ρ_c at 31.4°C, 36.3°C and 45.2°C. For the sake of completeness, the experimental data presented in this figure are reported also in Table 1. All the isotherms exhibit a similar behavior: the excess amount adsorbed first increases to reach a maximum value and

Table 1 Experimental excess adsorption data of CO₂ on activated carbon Filtrasorb 400. The data between brackets are not reliable enough since they have been measured at conditions too close to the critical point

| <i>T</i> (K) | ρ (g/L) | n^{ex} (mmol/g) | <i>T</i> (K) | ρ (g/L) | n^{ex} (mmol/g) | <i>T</i> (K) | ρ (g/L) | n^{ex} (mmol/g) |
|--------------|--------------|-------------------|--------------|--------------|-------------------|--------------|--------------|-------------------|
| 304.6 | 887.2 | 1.80 | | 12.9 | 5.07 | | 30.1 | 6.30 |
| | 857.7 | 2.00 | | 6.2 | 3.71 | | 16.3 | 5.20 |
| | 809.8 | 2.35 | 309.5 | 854.6 | 2.00 | | 7.4 | 3.76 |
| | 770.7 | 2.66 | | 807.3 | 2.33 | 318.4 | 785.5 | 2.39 |
| | 722.1 | 3.08 | | 757.7 | 2.71 | | 731.1 | 2.81 |
| | 662.3 | 3.62 | | 701.9 | 3.18 | | 679.0 | 3.22 |
| | 588.4 | 4.34 | | 658.3 | 3.57 | | 611.9 | 3.83 |
| | (548.5) | (4.70) | | 607.9 | 4.06 | | 558.6 | 4.31 |
| | (521.3) | (4.89) | | 555.4 | 4.58 | | 508.6 | 4.78 |
| | (492.9) | (5.14) | | 519.7 | 4.95 | | 454.5 | 5.31 |
| | (466.2) | (5.37) | | 457.2 | 5.61 | | 437.2 | 5.46 |
| | (433.3) | (5.85) | | 413.0 | 6.05 | | 425.1 | 5.57 |
| | 403.1 | 6.39 | | 375.5 | 6.40 | | 366.5 | 6.09 |
| | 368.7 | 6.81 | | 335.5 | 6.74 | | 303.0 | 6.60 |
| | 307.3 | 7.33 | | 288.3 | 7.12 | | 209.8 | 7.19 |
| | 244.4 | 7.74 | | 242.6 | 7.40 | | 167.2 | 7.35 |
| | 180.7 | 8.03 | | 194.5 | 7.65 | | 129.4 | 7.40 |
| | 145.7 | 8.10 | | 162.7 | 7.76 | | 85.6 | 7.22 |
| | 111.9 | 8.07 | | 136.0 | 7.79 | | 47.9 | 6.58 |
| | 74.6 | 7.83 | | 107.1 | 7.75 | | 28.8 | 5.78 |
| | 49.8 | 7.39 | | 79.7 | 7.57 | | 14.9 | 4.60 |
| | 28.2 | 6.51 | | 51.8 | 7.12 | | 7.8 | 3.45 |

Fig. 8 Excess adsorption isotherms of CO₂ on activated carbon as a function of the reduced density ρ^b/ρ_c measured at three different temperatures. Configuration PU, temperatures 31.4°C, 36.3°C and 45.2°C



then decreases almost linearly at increasing reduced density. In general, the lower the temperature, the larger the excess amount adsorbed; this effect is evident below the critical density of the fluid, where the three isotherms can be clearly distinguished, but it is also present though less evident above the critical density, where the isotherms get close to each other. An exception to the general trend is observed near the critical temperature and the critical density. At reduced density values between 0.9 and 1.2, the measured values of the excess amount adsorbed at 31.4°C are in fact smaller than or equal to those at 36.3°C. Similar effects have been observed previously for other experimental systems, and have been called “critical depletion” (Machin, 1999; Rajendran et al., 2002; Thommes et al., 1994, 1995). Such phenomenon has always eluded a convincing theoretical explanation. Based on the analysis reported in this work, we believe that under the conditions where the 31.4°C and 36.3°C isotherms cross over, the measurement accuracy is too low to make it possible to draw any positive conclusion about the reason of the cross-over itself. We cannot rule out that this is indeed a real physical phenomenon that could be considered an occurrence of “critical depletion”. However, the experimental error under those conditions is so large to justify also the conclusion that the observed cross-over is actually an experimental artifact. This dilemma cannot be solved with the experimental technique utilized in this work. Therefore, we conclude that the measured adsorption data are reliable under all conditions but under those too close to the critical point of CO₂, where the experimental error is too large, as discussed earlier. This is highlighted in Table 1, where the unreliable data are put between brackets. We believe that the measurements without adsorbent presented in this work represent a reliable, effective and simple procedure to assess for any new system under which conditions the adsorption measurements are accurate enough.

4 Conclusion

This work highlights once more the challenging task of measuring high pressure excess adsorption isotherms, especially in the near-critical region. It has been shown that the presence of temperature gradients inside the measuring cell leads to errors in the measurement of the excess adsorption. An improvement is achieved by optimizing the device thermostating system, namely

by changing the position of the inlet fluid. By testing these different arrangements an optimal configuration has been found. An approach has also been given to correct a posteriori the measured isotherms, based on the use of a kind of calibration measurement carried out without adsorbent. Even though the approach is effective, the adoption of a configuration which leads to negligible density gradients inside the measuring cell is believed to be the best experimental approach and to eliminate the need of further experiments without adsorbent. Finally, the selected configuration has been used to study the adsorption of CO₂ on activated carbon Filtrasorb 400. As expected the measuring technique leads to a successful description of the adsorption behavior. Even though representing a step forward, these results confirm that the accuracy of the gravimetric technique should be further improved when measurements in the very vicinity of the critical point are carried out.

Nomenclature

| | |
|------------------|---|
| m_{ads} | Adsorbent mass (g) |
| M_{m} | Molar mass of adsorbate (g/mol) |
| \mathcal{M}_1 | Mass at measuring point 1 (g) |
| \mathcal{M}_2 | Mass at measuring point 2 (g) |
| n^{ex} | Molar excess adsorption per adsorbent mass (mmol/g) |
| T | Temperature (K) |
| V | Volume (cm ³) |
| P | Pressure (bar) |

Greek Letters

| | |
|--------------|--|
| Γ | Adsorption excess in mass units (g) |
| Γ^* | Fictitious adsorption excess in mass units (g) |
| ρ | Density (g/cm ³) |
| $\Delta\rho$ | Density difference (g/cm ³) |
| ϵ | Relative density error (-) |

Subscripts and Superscripts

| | |
|-----|-----------------------------------|
| 0 | Solid parts in the measuring cell |
| ads | Adsorbent |
| b | Bulk |
| c | Critical |
| He | Helium |
| Sk | Sinker |
| B | Basket |

Acknowledgments Partial support of the Swiss National Science Foundation through grant NF 200020-107657/1 is gratefully acknowledged.

References

- Di Giovanni, O., W. Dörfler, M. Mazzotti, and M. Morbidelli, “Adsorption of Supercritical Carbon Dioxide on Silica,” *Langmuir*, **17**, 4316–4321 (2001).
- Dreisbach, F. and H.W. Lösch, “Magnetic Suspension Balance for Simultaneous Measurement of a Sample and the Density of the Measuring Fluid,” *Journal of Thermal Analysis and Calorimetry*, **62**, 515–521 (2000).
- Hocker, T., A. Rajendran, and M. Mazzotti, “Measuring and Modeling Supercritical Adsorption in Porous Solids. Carbon Dioxide on 13X Zeolite and on Silica Gel,” *Langmuir*, **19**, 1254–1267 (2003).
- Humayun, R. and D.L. Tomasko, “High-Resolution Adsorption Isotherms of Supercritical Carbon Dioxide on Activated Carbon,” *AIChE*, **46**, 2065–2075 (2000).
- Kiselev, S.B. and J.F. Ely, “Simplified Crossover Droplet Model for Adsorption of Pure Fluids in Slit Pores,” *Journal of Chemical Physics*, **120**, 8241–8252 (2004).
- Kiselev, S.B., J.F. Ely, and M.Y. Belyakov, “Adsorption of Critical and Supercritical Fluids,” *Journal of Chemical Physics*, **112**, 3370–3383 (2000).
- Kiselev, S.B., L. Lue, and M.Y. Belyakov, “Universal Crossover Function and Non-Universal Order-Parameter Profiles for Critical Adsorption,” *Physics Letters A*, **260**, 168–168 (1999).
- Machin, W.D., “Properties of Three Capillary Fluids in the Critical Region,” *Langmuir*, **15**, 169–173 (1999).
- Maciolek, A., A. Ciach, and R. Evans, “Critical Depletion of Fluids in Pores: Competing Bulk and Surface Fields,” *Journal of Chemical Physics*, **108**, 9765–9774 (1998).
- Maciolek, A., R. Evans, and N.B. Wilding, “Effects of Confinement on Critical Adsorption: Absence of Critical Depletion for Fluids in Slit Pores,” *Physical Review E*, **60**, 7105–7119 (1999).
- Ottiger, S., R. Pini, A. Rajendran, G. Storti, and M. Mazzotti, *Study of Adsorption of Supercritical Carbon Dioxide on Carbon-Based Adsorbents*, Presented at International Symposium on Supercritical Fluids, Orlando, 2005.
- Rajendran, A., T. Hocker, O.D. Giovanni, and M. Mazzotti, “Experimental Observation of Critical Depletion: Nitrous Oxide Adsorption on Silica Gel,” *Langmuir*, **18**, 9726–9734 (2002).
- Schoen, M. and M. Thommes, “Microscopic Structure of a Pure Near-Critical Fluid Confined to a Mesoscopic Slit-Pore,” *Physical Review E*, **52**, 6375–6386 (1995).
- Schoen, M., M. Thommes, and G.H. Findenegg, “Aspects of Sorption and Phase Behavior of Near-Critical Fluids Confined to Mesoporous Media,” *Journal of Chemical Physics*, **107**, 3262–3266 (1997).
- Sircar, S., “Measurement of Gibbsian Surface Excess,” *AIChE*, **47**, 1169–1176 (2001).
- Thommes, M., G.H. Findenegg, and H. Lewandowski, “Critical Adsorption of SF₆ on a Finely Divided Graphite Substrate,” *Berichte Der Bunsen-Gesellschaft-Physical Chemistry Chemical Physics*, **98**, 477–481 (1994).
- Thommes, M., G.H. Findenegg, and M. Schoen, “Critical Depletion of a Pure Fluid in Controlled-Pore Glass - Experimental Results and Grand-Canonical Ensemble Monte-Carlo Simulation,” *Langmuir*, **11**, 2137–2142 (1995).
- Wilding, N.B. and M. Schoen, “Absence of Simulation Evidence for Critical Depletion in Slit Pores,” *Physical Review E*, **60**, 1081–1083 (1999).